Alternatively Folded States of an Immunoglobulin

Johannes Buchner, Michael Renner, Hauke Lilie, Hans-Jürgen Hinz, and Rainer Jaenicke*
Institut für Biophysik and Physikalische Biochemie, Universität Regensburg, Universitätsstraße 31, D-8400 Regensburg, FRG
Thomas Kiefhaber
Laboratorium für Biochemie, Universität Bayreuth, Postfach, D-8580 Bayreuth, FRG
Rainer Rudolph*
Boehringer Mannheim GmbH, Biochemical Research Center, Nonnenwald 2, D-8122 Penzberg, FRG
Received February 14, 1991; Revised Manuscript Received April 11, 1991

ABSTRACT: Well-defined, non-native protein structures of low stability have been increasingly observed as intermediates in protein folding or as equilibrium structures populated under specific solvent conditions. These intermediate structures, frequently referred to as *molten globule* states, are characterized by the presence of secondary structure, a lack of significant tertiary contacts, increased hydrophobicity and partial specific volume as compared to native structures, and low cooperativity in thermal unfolding. The present study demonstrates that under acidic conditions (pH < 3) the antibody MAK33 can assume a folded stable conformation. This A-state is characterized by a high degree of secondary structure, increased hydrophobicity, a native-like maximum wavelength of fluorescence emission, and a tendency toward slow aggregation. A prominent feature of this low-pH conformation is the stability against denaturant and thermal unfolding that is manifested in highly cooperative reversible phase transitions indicative of the existence of well-defined tertiary contacts. These thermodynamic results are corroborated by the kinetics of folding from the completely unfolded chain to the alternatively folded state at pH 2. The given data suggest that MAK33 at pH 2 adopts a cooperative structure that differs from the native immunoglobulin fold at pH 7. This *alternatively folded state* exhibits certain characteristics of the *molten globule* but differs distinctly from it by its extraordinary structural stability that is characteristic for native protein structures.

The central idea of protein folding states that a distinct amino acid sequence specifies only one three-dimensional conformation, the native state, which is characterized by optimized secondary and tertiary interactions. The stability of the native structure results from hydrogen bonds, as well as polar, van der Waals, and hydrophobic interactions (Dill, 1990; Privalov & Gill, 1988). The specific nature of these interactions is manifested in the occurrence of highly cooperative unfolding transitions, once certain limiting environmental parameters have been surpassed. In contrast, the denatured state is devoid of ordered and stable intramolecular contacts (Privalov, 1979; Privalov & Gill, 1988; Jaenicke, 1987, 1991). The structural transitions accompanying renaturation seem to follow distinct pathways. The precise mechanism of structure formation is still enigmatic. It is, however, known from detailed kinetic analyses of model proteins such as basic pancreatic trypsin inhibitor, ribonuclease, or cytochrome *c* that specific kinetic intermediates with a relatively high degree of native-like secondary structure occur as early precursors in the folding reaction (Kim & Baldwin, 1990).

Since folding intermediates of a number of monomeric proteins show common characteristics, the term *molten globule* has been coined as a general term for these conformational states (Kuwajima, 1989). Similar structural states have been observed under equilibrium conditions, e.g., at low or high pH, high temperature, or moderate concentrations of denaturant (Kuwajima et al., 1981; Kronman et al., 1965, 1967; Mulqueen & Kronman, 1982; Dolgikh et al., 1985; Damaschun et al., 1986; Gast et al., 1986). The *molten globule* state is characterized by (i) a high degree of secondary structure, (ii) the absence of tertiary contacts, (iii) solvent accessibility of hydrophobic residues, (iv) an increased volume compared to the native state, (v) low cooperativity in thermal- or denaturant-induced unfolding transitions, and (vi) a rapid equilibrium with the denatured state. The anion-induced structure formation of the *molten globule* state at acidic pH has been investigated in detail by Goto et al. (1990a,b). In the case of β-lactamase, cytochrome *c*, and apomyoglobin, anions have to be present to induce the formation of a significant amount of secondary structure at low pH values (Goto et al., 1990a,b). Since the *molten globule* state has been detected in the folding pathway of many different proteins, and since the conditions that induce the formation of this state are apparently diverse, the term seems to describe a large number of conformationally related states (Kuwajima, 1989; Baldwin, 1990; Jaenicke, 1991).

In order to investigate whether alternatively folded states different from the *molten globule* could exist, we chose immunoglobulin as a model system. The structure, folding, and stability of immunoglobulins and their fragments are well characterized (Goto et al., 1979, 1987; Goto & Hamaguchi, 1982; Kikuchi et al., 1986; Tsunegawa et al., 1987). Furthermore, antibodies show a high degree of internal structural homology. The individual domains are characterized by a repetitive structural motif, the so-called immunoglobulin fold consisting of β-stranded sheets arranged in two layers (Amzel & Poljak, 1979; Davies & Metzger, 1983). No α-helical elements are present in native antibodies. This relatively simple folding pattern with only one kind of secondary and tertiary structural motif should facilitate the interpretation of structural changes.

† This work was supported by grants from the Deutsche Forschungsgemeinschaft (to R.J. and H.-J.H.) and the Fonds der Chemischen Industrie and by a DECHEMA biotechnology grant to J.B.
* To whom correspondence should be addressed.

0006-2960/91/0430-6922$02.50/0

In the present study we observed that the antibody MAK33[1] adopts a structural state at acidic pH that is different from both the native and the denatured states. We call this conformation an "alternatively folded state". The most conspicuous feature of this state is the presence of tertiary interactions that are reflected in the existence of reversible cooperative unfolding transitions. Such transitions are not compatible with a *molten globule* structure.

Materials and Methods

MAK33, a murine antibody of subtype κ/IgG1, was obtained from Boehringer Mannheim GmbH. The concentration of the antibody was determined spectrophotometrically at 280 nm, with A_{1cm} = 1.5 for a 0.1% solution. The extinction coefficient was calculated from the content of aromatic amino acids according to Wetlaufer (1962). The UV absorbance coefficients at pH 7 and pH 2 were identical within the limits of experimental error.

Adjustment of the antibody solution to pH 2 was achieved either by dialysis or by dilution. Unless indicated otherwise, the potassium phosphate buffer was adjusted to pH 2 with HCl. Therefore, the buffer solutions typically contained 50 mM chloride.

Spectroscopic Techniques. Corrected fluorescence spectra and fluorescence kinetics were recorded with use of a Hitachi F 4000 fluorescence spectrophotometer equipped with a magnetic stirrer. The excitation wavelength was 278 nm, and the bandwidth for excitation and emission was 5 nm. The protein concentration was 100 μg/mL. Folding kinetics were monitored by the change in fluorescence at 330 nm after excitation at 278 nm. The slits were set to 1.5 nm for excitation and 10 nm for emission. Native or denatured IgG was diluted into 40 mM potassium phosphate, pH 2, at 25 °C in 1-cm cells with a magnetic stirrer. The kinetics were analyzed with use of the programs Kinfit and Grafit.

CD spectra were recorded in a JASCO J-600A spectropolarimeter at protein concentrations of 0.6–1.0 mg/mL in 0.1-mm cells (peptide CD) or 1-mm cells (aromatic CD).

Thermal transition curves were monitored by the change in absorbance at 287 nm with use of a Gilford 2400S spectrophotometer equipped with a 2527 thermoprogrammer and a special cell of 1-cm light path. The protein concentration employed was 0.25 mg/mL, and the heating rate was 1 deg/min. Reversibility of the unfolding transition was assured by repeated heating and cooling cycles.

Dye Binding. The fluorescent dye Nile Red was obtained from Eastman-Kodak. The polarity-sensitive probe binds preferentially to hydrophobic regions of proteins. This leads to a blue shift in fluorescence emission as well as to an increase in quantum yield (Sackett & Wolff, 1987). MAK33 (1 μM) was incubated in potassium phosphate buffer together with Nile Red (1 μM) for 15 min at room temperature. Emission spectra (560–720 nm) were recorded in a Hitachi F 4000 fluorescence spectrophotometer. Excitation was at 550 nm. Spectra were corrected for buffer without Nile Red.

Densitometric Measurements. The partial specific volume of MAK33 at pH 2 was determined as previously described (Koynova & Hinz, 1990). Density differences between the protein solution and the buffer were recorded every 0.1 deg by use of two DMA 602 HT external cells connected to a DMA 60 measuring unit in the phase-lock loop mode (A. Paar, Graz, Austria). Temperature scans were performed by employing a Haake PG20 temperature controller and a Haake F3 thermostated bath. Protein concentration was 12 mg/mL.

Ultracentrifugation. Sedimentation velocity and sedimentation equilibrium runs were performed in an analytical ultracentrifuge (Beckman Spinco Model E) equipped with a high-sensitivity UV scanning system. Double-sector cells (12 mm) with sapphire windows were used at 36 000 and 12 000 rpm in an AnG rotor. Meniscus-depletion high-speed sedimentation equilibria (Yphantis, 1964) were evaluated by use of a computer program kindly provided by G. Böhm (University of Regensburg). Data were corrected for water viscosity and 20 °C; in the case of extreme pH values, charge effects on the partial specific volume were taken into consideration (Svedberg & Pedersen, 1940).

Calorimetric Measurements. Variation of the apparent heat capacity with temperature was measured with use of an electronically modified differential scanning microcalorimeter DASM-4 (Privalov et al., 1975; Moses & Hinz, 1983). Heat capacity and temperature data were numerically collected every 0.1 deg, employing a Keithley 192 analog to digital converter.

Each measurement with protein was preceded by a buffer run, to establish the base line and the calibration constant. Typically, measurements were started at 20 °C and carried out up to 90 °C. Heating rates of 1 and 2 K/min gave identical transition curves. In order to avoid vaporization, all measurements were performed under an excess pressure of 2.5 bar.

The buffer used was 40 mM potassium phosphate. Before each measurement, the protein was dialyzed overnight in at least a 1000-fold excess of buffer. Protein concentrations between 1.5 and 3.0 mg/mL were used in the measurements.

For the evaluation of the enthalpy from the heat capacity vs temperature curves, two programs were routinely employed: (i) overall enthalpies were determined by numerical integration of the transition peak or (ii) deconvolution of the heat capacity curves into sequential subtransitions was performed by use of the deconvolution algorithm of Freire and Biltonen (1978). The corresponding programs were written by M. Renner (1991).

The van't Hoff enthalpies of the two-state subtransitions were calculated from the calorimetric data according to eq 1,

$$\Delta H_{vH} = 4RT_m^2 \frac{\Delta C_p(T_m)}{\Delta H_{cal}(T_m)} \quad (1)$$

where T_m is the temperature at 50% unfolding of the protein, $\Delta C_p(T_m)$ is the heat capacity at T_m, and $\Delta H_{cal}(T_m)$ is the calorimetric enthalpy at T_m. Molar values of the thermodynamic parameters have been calculated on the basis of a molecular mass of 150 kDa.

Results

The A-State of MAK33 Differs from Both the Native and the Denatured State. In order to determine the secondary structure, CD spectra of native, GdmCl-denatured, and "acid-denatured" (A-state) MAK33 were recorded in the far-UV range (i.e., 185–250 nm). While antibody denatured by GdmCl exhibits the typical spectrum of a random-coil polypeptide, both the native protein and the A-state show spectra characteristic for proteins with secondary structure (Figure 1A). Surprisingly, the acidic form reveals a stronger negative ellipticity than the native protein. This implies that large structural rearrangements must have taken place in the antibody molecule upon acidification. CD spectra in the

[1] Abbreviations: A-state, conformational state achieved at acidic pH; CD, circular dichroism; CK-MM, human muscle-type creatine kinase; DSC, differential scanning calorimetry; GdmCl, guanidinium chloride; MAK33, murine antibody of subclass IgG1, directed against CK-MM.

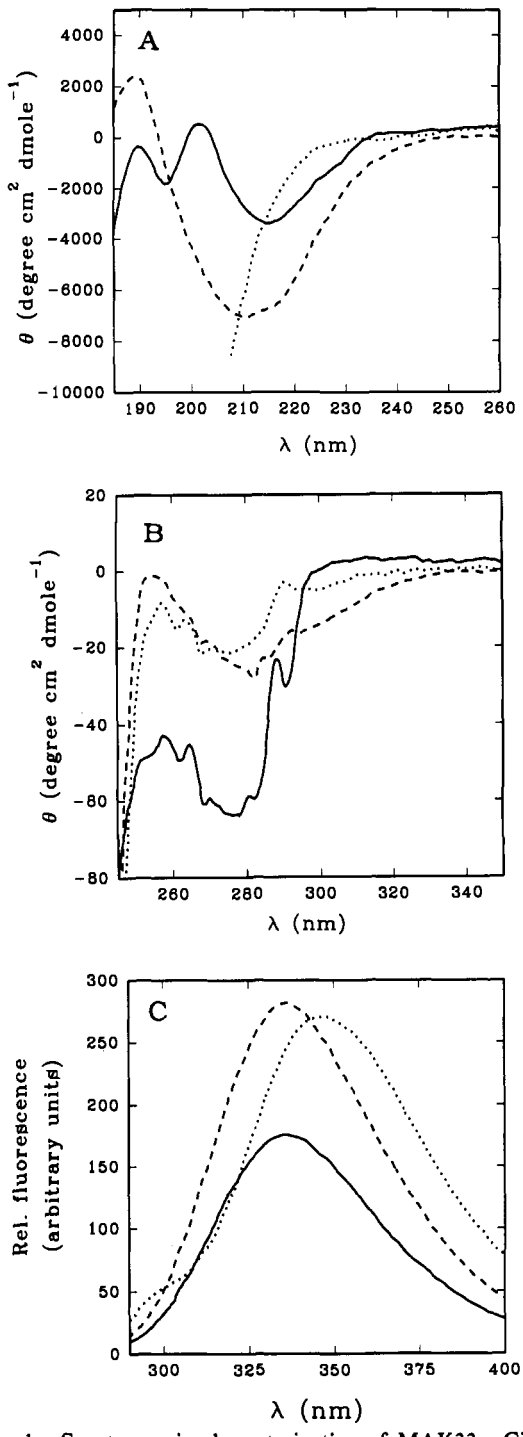

FIGURE 1: Spectroscopic characterization of MAK33. Circular dichroism and fluorescence spectra were recorded in 40 mM potassium phosphate, pH 7 (—), 40 mM potassium phosphate pH 7, 6 M GdmCl (···), and 40 mM potassium phosphate, pH 2 (---). (A) Variation of the molar ellipticity with wavelength in the peptide region. (B) Variation of the molar ellipticity with wavelength in the aromatic region. (C) Fluorescence emission.

near-UV range (i.e., 240–350 nm) show that the A-state is different from both the denatured and the native state (Figure 1B). The observed ellipticities indicate differences in the asymmetric environment of the aromatic amino acids in the A-state as compared to that of the native protein.

Fluorescence emission spectra of native, denatured, and A-state antibody show that aromatic residues are in an environment with similar polarity both in the native and the A-state. The wavelength of maximum fluorescence emission is 335 nm in both cases (Figure 1C). The fluorescence intensities of the denatured and the acidic form are significantly higher than that of the native state, probably because of a fluorescence quench by disulfide bridges adjacent to tryptophans in the native state (Cowgill, 1967; Tsunegawa, 1987). Both incubation in GdmCl and incubation in acid result in a spatial separation of disulfide bridges and aromatic amino acids.

Table I: Determination of the Sedimentation Coefficient and Molecular Mass of MAK33 in 40 mM Potassium Phosphate at 20 °C[a]

pH	$s_{20,solv}$ (S)	$s_{20,w}$ (S)	mass (kDa)
2.0	6.03 ± 0.02	5.53 ± 0.02	164.2 ± 6.0
2.7	6.14 ± 0.02	5.72 ± 0.02	
4.2	6.60 ± 0.09	6.49 ± 0.09	
4.7	6.61 ± 0.09	6.48 ± 0.09	
7.0	6.60 ± 0.04	6.60 ± 0.04[b]	153.8 ± 3.4
11.9	6.12 ± 0.04	5.58 ± 0.04	
12.2	6.07 ± 0.11	5.53 ± 0.11	
2.0[c]	3.0 ± 0.5	3.2 ± 0.5	152.0 ± 8.0

[a] Sedimentation coefficients were calculated from log r vs t plots and corrected according to Svedberg and Pedersen (1940). [b] For pH 7, extrapolation of $s_{20,w}$ to zero concentration yielded $s^0_{20,w}$ = 6.93 S. [c] In 6 M GdmCl.

MAK33 Immunoglobulin in the A-State Is a Compact Monomer. As shown by analytical ultracentrifugation, pH changes cause prominent effects on the hydrodynamic properties of IgG (Table I). The decrease at extreme net charge becomes even more significant after correcting the sedimentation rate for solvent viscosity, temperature, density, and charge effects on the partial specific volume. Densitometric determination of the latter at 20 °C yields 0.719 $cm^3\ g^{-1}$ at pH 2 and 0.735 $cm^3\ g^{-1}$ at pH 7, respectively. Differences in the sedimentation coefficients may be attributed to changes in hydration or in the shape of the molecule. Compared to the much more drastic effect of chaotropic agents, the protein in its A-state and at alkaline pH preserves its compact globular character. As one would expect, the molecular mass is affected neither by pH nor by additives causing denaturation: high-speed sedimentation equilibrium runs at 12000 rpm yield masses of 153.8 ± 3.4 kDa (pH 7) and 164.2 ± 6 kDa (pH 2).

While the protein at neutral pH is homogeneous (correlation coefficient > 0.999 over the whole concentration range in the ln c vs r^2 diagram), the protein in its A-state shows slow aggregation. After 16 h of dialysis, the plateau of the initial concentration yields only ~80% of its theoretical value, corresponding to about 20% aggregation. Due to the low rate of aggregation, the sedimentation analysis is not significantly perturbed, even in the case of high-speed sedimentation equilibria.

The sedimentation coefficients at acid and alkaline pH signal similar alterations in the hydrodynamic properties of immunoglobulin. This observation seems to contradict the different conformational properties of the molecule reflected by its dichroic absorbance at pH 2 and pH 12. However, in comparing the two sets of data, one has to keep in mind that charge effects on the shape and hydration of proteins and their constituent domains are not necessarily connected with conformational changes or alterations in the environment of chromophores.

Hydrophobic Amino Acids Are Solvent Accessible. Binding experiments with the polarity-sensitive dye Nile Red (Sackett & Wolff, 1987) were performed in order to investigate the relative hydrophobicity of the accessible protein surface of the different conformational states. At pH 2, the A-state of MAK33 binds Nile Red, as shown by both a shift of the

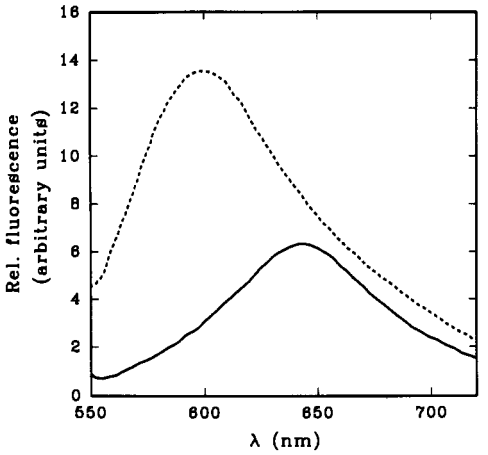

FIGURE 2: Accessibility of hydrophobic residues of MAK33 at pH 7 and pH 2 as determined by Nile Red fluorescence. MAK33 (100 μM) in H_2O was diluted 100-fold in potassium phosphate adjusted to pH 7 or pH 2. Incubation with Nile Red was for 15 min. Excitation wavelength was 550 nm. Spectra for MAK33 plus Nile Red at pH 7 (—) and pH 2 (---) are corrected for buffer without Nile Red.

wavelength of maximum emission from 650 nm (for the unbound dye) to 605 nm (for the dye bound to the A-state) and an increase in the fluorescence intensity (Figure 2). The native antibody does not interact with Nile Red. The maximum emission wavelength of Nile Red in buffer alone or in buffer containing the native protein is the same, and the difference in fluorescence intensity is small. Thus, the structural changes associated with incubation at acidic pH result in an increased accessibility of hydrophobic amino acids to the solvent.

The Folding Processes Leading to the A-State Comprise Both Slow and Fast Kinetics. The structural transition from the native state at pH 7 to the A-state at pH 2 was initiated by diluting an aqueous protein solution (pH 7) into pH 2 buffer. The dilution factor was 150. Since there is a marked difference in the intensity of fluorescence emission between the native state and the A-state (Figure 1C), fluorescence kinetics were monitored at 330 nm (Figure 3A). The kinetics of folding are complex. Three slow phases can be well resolved in a kinetic analysis of the folding curves. The rates of all steps are independent of the protein concentrations employed. Therefore, all reactions seem to be first-order folding processes. Aggregation and/or association processes can be ruled out as the molecular origin of the observed kinetics. Analysis of the curves gives relaxation times of 1800, 400, and 25 s for the three slow phases at 25 °C. The sum of the amplitudes of the folding steps comprises the total differences in fluorescence between the native state and the A-state (Figure 1C), so that fast processes do not seem to occur within the dead time of mixing.

The folding transition from the native state to the A-state is not reversible since the protein in its A-state aggregates very rapidly and irreversibly upon dilution from pH 2 to pH 7.

Folding kinetics from the unfolded state in 6 M GdmCl, pH 2, to the A-state were performed by diluting denatured MAK33 IgG 100-fold into 40 mM potassium phosphate, pH 2. In contrast to the folding reactions starting from the native state at pH 7, the refolding from the denatured state comprises both fast and slow reactions (Figure 3B). About 85% of the fluorescence change occurs within the dead time of mixing (1 s) while 15% of the signal is regained with relaxation times of 1100, 60, and 8 s, respectively. Light scattering shows that aggregation processes did not occur during the time course of structure formation.

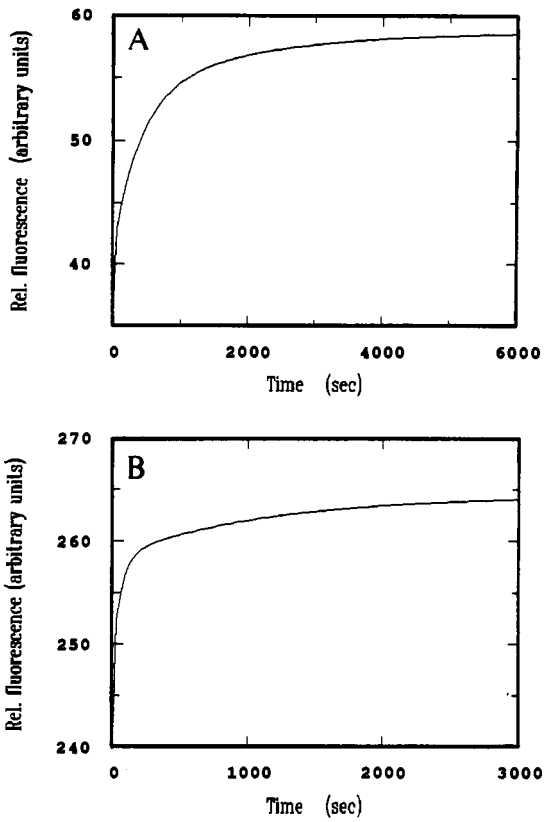

FIGURE 3: Kinetics of acid-induced folding of MAK33 at 25 °C. (A) Structural transition from the native state to the A-state. Native antibody in 40 mM potassium phosphate, pH 7, was diluted 150-fold in 40 mM potassium phosphate, pH 2. The final antibody concentration was 67 μg/mL. Kinetic analysis of the data gives first-order relaxation times of 1800, 400, and 25 s; the corresponding amplitudes are 59, 13, and 28%, respectively. (B) Folding kinetics from the unfolded state to the A-state. Denatured antibody in 6 M GdmCl, pH 2, was diluted 100-fold in 40 mM potassium phosphate, pH 2. The final antibody concentration was 100 μg/mL. Apart from a very fast phase (85% of the total amplitude), three slow first-order reactions can be resolved (15% of the total amplitude) with relaxation times of 1100, 60, and 8 s, respectively.

The Structural Changes Are Followed by Salt-Dependent Slow Aggregation Processes. Since the hydrophobicity of the antibody in the A-state is increased compared to the in native state, the protein tends to aggregate. Light scattering at 500 nm was used to follow aggregation during the reshuffling process after the dilution of antibodies from the native state (pH 7) to pH 2. The aggregation processes observed are slower by several orders of magnitude than the kinetics of folding/reshuffling at acidic pH: aggregation proceeds for days without reaching a plateau.

The extent of aggregation observed at pH 2 by light scattering is markedly influenced by the concentration of NaCl present in the solution. Relative intensities after 25 h of incubation at pH 2 as a function of salt concentration are shown in Figure 4. Up to about 250 mM NaCl, a slight increase in aggregation is observed, while at higher concentrations the protein is significantly aggregated.

The Acid Form Is Remarkably Stable against GdmCl-Induced Denaturation. To obtain a measure of the relative stability and cooperativity of the A-state, the equilibrium transition from the folded A-state at pH 2 to the unfolded conformation induced by the addition of GdmCl and the respective reverse transition were monitored by fluorescence measurements (Figure 5). The transition is completely reversible over the whole transition range. The pronounced sigmoidal shape of the transition curve is indicative of a co-

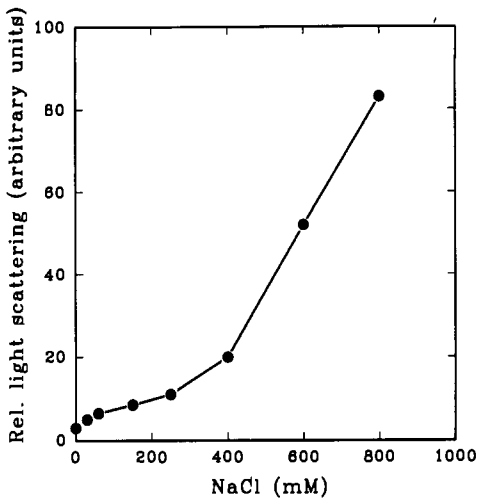

FIGURE 4: Salt dependence of the aggregation of MAK33 at pH 2. Native antibody in H_2O was diluted into 40 mM potassium phosphate, pH 2. Light scattering was detected at 360 nm after 25 h of incubation at 25 °C. Antibody concentration was 100 μg/mL.

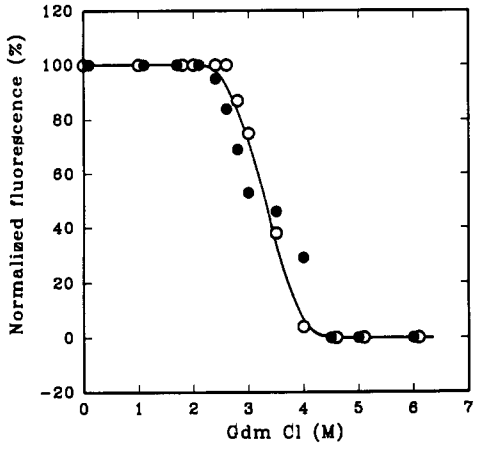

FIGURE 5: GdmCl-induced denaturation of MAK33 from its A-state at pH 2 (○) and renaturation of MAK33 from 6 M GdmCl pH 2 (●). The protein was diluted in 40 mM potassium phosphate, pH 2, containing 0–6 M GdmCl. Fluorescence emission at 335 nm was recorded after 20 h of incubation at 20 °C and normalized according to Pace (1986). Protein concentration was 100 μg/mL; excitation was at 278 nm.

operative folding process. The observed pattern is typical for proteins with a high amount of tertiary contacts.

Thermal Denaturation Shows Highly Cooperative and Reversible Unfolding of the A-State. Thermal denaturation was also used to study the cooperativity and reversibility of the denaturation processes. Unfolding was monitored by the temperature-dependent change in absorbance at 287 nm. The transition curve at pH 2 (data not shown) exhibits perfect reversibility as demonstrated by repeated heating and cooling cycles. In contrast, thermal denaturation of the native antibody at pH 7 is irreversible.

To obtain quantitative energy parameters for the different structures, calorimetric measurements were performed at various pH values. While the transitions observed below pH 3 are reversible, transitions at higher pH values are irrevesible by the calorimetric criterion that the second heating does no longer show an excess heat capacity peak. Despite this irreversibility, thermodynamic analysis can be applied to these processes as outlined by Sturtevant (1987) and Brandts and Lin (1990), if the phenomena causing irreversibility are much slower than the unfolding transition. This criterion is met with the present system.

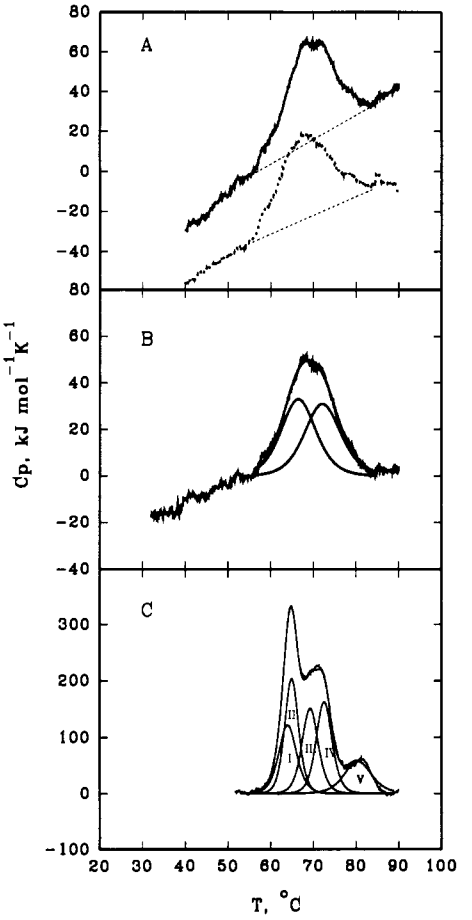

FIGURE 6: DSC transition curves of MAK33 at pH 2 and pH 7. Heating rate was 1 K/min. The base lines used for enthalpy determination are indicated by dashed lines. (A) pH 2.0; protein concentration 1.0 mg/mL. The dotted curve represents the transition profile of the second heating. (B) Deconvolution of the curve shown in (A) into sequential two-state transition curves. (C) pH 7.0; protein concentration 1.3 mg/mL.

Table II: Thermodynamic Parameters for the Reversible Transitions of MAK33 at Different pH Values from DSC Measurements[a]

pH	T_m (°C)	ΔH (kJ/mol)	Δh (J/g)
2.0	66.5	355	4.7
	72.1	347	
2.7	65.6	346	4.7
	73.4	378	
7.0	63.9	684	24.2
	64.9	883	
	69.2	773	
	72.5	806	
	80.4	497	

[a] The enthalpies and transition temperatures result from a deconvolution of the excess heat capacity curves into sequential two-state transitions.

Figure 6 exhibits typical DSC curves of IgG at pH 2 and pH 7. The dotted transition curve in Figure 6A shows a second run with the same sample. The reproducibility of the excess heat capacity function demonstrates the reversibility of the unfolding transition at pH 2. The shape of the heat capacity curve is suggestive of a multistate behavior. Quantitative deconvolution of the transition curve (Renner, 1991) yields two all-or-none transitions, as shown in Figure 6B. The corresponding thermodynamic parameters are summarized in Table II. It can be seen that at pH 7 the magnitude of the specific transition enthalpy, Δh, is comparable to values obtained for other compact proteins. At pH 2, however, the strong decrease in the Δh value suggests a drastic reduction

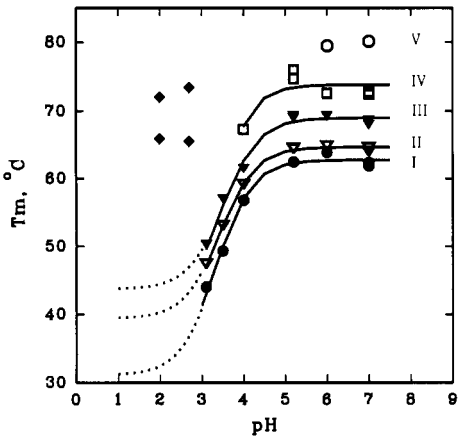

FIGURE 7: Variation with pH of the transition temperatures of the subtransitions shown in Figure 6C. The experimental T_m values were fitted to a titration curve with use of eq 2 (full lines). The roman numerals refer to the identically labeled subtransitions in Figure 6C. The new high-temperature transitions that appear at pH values below pH 2.7 are illustrated by ◆. The inflection points and the lower and upper transition temperatures are listed in Table III.

Table III: Parameters Derived from a Nonlinear Least-Squares Analysis of the pH Dependence of the Subtransitions Observed in MAK33[a]

peak no.	t_l (°C)	t_u (°C)	pK
I	31.1 ± 1.6	62.8 ± 0.4	3.35 ± 0.07
II	39.4 ± 1.3	64.7 ± 0.2	3.43 ± 0.05
III	43.7 ± 0.5	68.9 ± 0.4	3.52 ± 0.14
IV		73.2 ± 0.5	
V		82.2 ± 0.2	

[a] Parameters were derived according to eq 2 (cf. Figure 6).

in the number or strength of the intramolecular interactions. The Δh value is smaller by a factor of approximately 4 than the corresponding specific transition enthalpy of RNase A at pH 2.5. Multistate unfolding is quite obvious in the IgG transition curve at pH 7. The curve can be resolved in a unique manner into five sequential two-state transitions as indicated in Figure 6C. Attempts to fit the calorimetric profiles by four or six subtransitions lead to a significant decrease in the reduced χ^2 value (Bevington, 1969).

Figure 7 displays the variation with pH of the transition temperatures, T_m, of the five substransitions. These T_m values result from a series of microcalorimetric studies at different pH values. The corresponding theoretical curves (solid lines) for the pH dependence of T_m have been calculated on the basis of a least-squares procedure by use of eq 2 (Schwarz et al., 1987). t_u and t_l, the upper and lower transition temperatures, respectively, and the midpoint, pK, of the titration curve are variables in the minimization algorithm. Subtransition V of Figure 6C occurs only at pH 6 and 7. Therefore, it can only be deconvoluted at these two pH values. The T_m values of the remaining four peaks show practically no pH dependence down to pH 4.5. Between pH 4 and pH 3 there is a considerable decrease in all remaining T_m values, and, most remarkably, in this pH range subtransition IV vanishes as did subtransition V below pH 6.

$$T_m = \frac{t_l + t_u 10^{pH-pK}}{1 + 10^{pH-pK}} \quad (2)$$

The results obtained for t_u, t_l, and pK from these measurements are summarized in Table III. Disappearance of the subtransitions IV and V prevents the calculation of all relevant parameters for these transitions.

Independent of the numerical analysis of the data, the most remarkable finding of the calorimetric studies is the existence of a high-temperature transition peak at low pH values (2.7 and 2.0). This transition cannot be extrapolated from inspection of the T_m vs pH profiles (Figure 7). On the basis of these curves one would not expect any transitions with T_m values higher than 45 °C at pH 2. Therefore, one has to conclude that the decrease in pH results in the formation of a new, well-defined structure that does not exist at higher pH values. It can be unfolded reversibly (Figure 6A) and remains the only stable structure at a further decrease of pH.

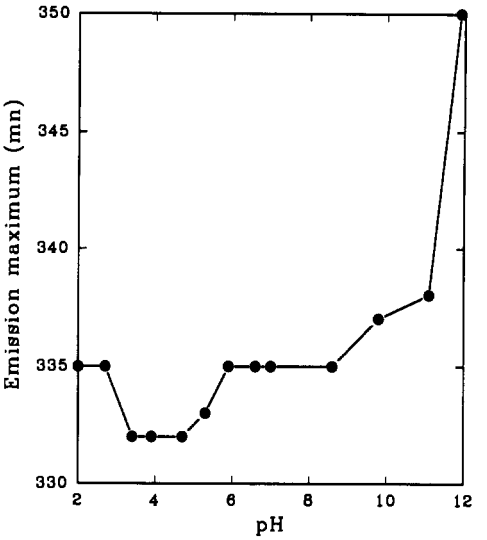

FIGURE 8: Dependence of the fluorescence emission maximum of MAK33 on pH. Native antibody was diluted into 40 mM potassium phosphate adjusted to pH values between pH 2 and pH 12. Fluorescence emission was recorded at 40 °C after 26 h of incubation at 25 °C and an additional 30 min of incubation at 40 °C. Protein concentration was 100 μg/mL; excitation wavelength was 278 nm.

The Alternatively Folded State Is Confined to Acidic pH. Protein fluorescence was monitored from pH 2 to pH 12 in orrder to investigate the conformational state of MAK33 over the whole pH range (Figure 8). From pH 6 to pH 9, the protein is in its native state, as shown by the wavelength of maximum emission and the relative fluorescence intensity. From pH 9 to pH 12, an unfolding transition is observed. At pH 12 the maximum emission wavelength is 350 nm, comparable to the wavelength observed in 6 M GdmCl (cf. Figure 1C).

The structural transition from the native state to the A-state is accompanied by an intermediate blue shift of the fluorescence emission from 335 nm at pH 7 to 332 nm between pH 5.0 and pH 3.5 (Figure 8). This blue shift is not accompanied by aggregation, since no increase in light scattering could be observed. Below pH 3.5, the wavelength of maximum fluorescence emission is restored to 335 nm. The fluorescence intensity increases drastically below pH 3.8 (data not shown). This increase, as well as the slight red shift of the maximum emission wavelength, may reflect the structural rearrangements leading to the alternatively folded state at pH 2.

Discussion

Acid-induced denaturation has been reported for a variety of proteins (Tanford, 1968). Although enzymatic activity is generally lost upon acidification, the conformational state adopted at low pH is in some cases different from the random coil obtained after denaturation with strong denaturants such as GdmCl (Rudolph et al., 1975; Jaenicke, 1987). Some proteins, such as γ II-crystallin and RNase T1, even retain their native conformation at acidic pH (Rudolph et al., 1990; Kiefhaber et al., 1990). There are other examples where the

negative ellipticity of the protein in the far-UV range is in part retained (Engelhard et al., 1976; Zettlmeissl et al., 1981; McCoy & Wong, 1981; Goloubinoff et al., 1989; Goto & Fink, 1989). In addition, there are proteins like the *Pseudomonas* exotoxin A that at acidic pH adopt a functional conformation differing from that of the native protein (Jiang & London, 1990).

Acid-specific structures that show as common properties salt-dependent secondary structure, no significant tertiary contacts, exposure of hydrophobic residues, increased partial specific volume, and low cooperativity in thermal unfolding are referred to as *molten globule* states (Ptitsyn, 1987; Kuwajima, 1989; Ptitsyn et al., 1990). Intermediates of protein folding frequently exhibit similar structural properties. However, the present study has shown that also under acidic conditions other stable but non-native structures such as the A-state of IgG can occur. The analysis of this alternative structure may be instrumental in providing additional information on the intricate mechanism of protein structure formation.

So far, detailed studies on the nature of the A-state have been confined to small monomeric proteins. In order to extend the investigations to larger proteins we chose a murine monoclonal antibody (MAK33) (Buckel et al., 1987; Buchner & Rudolph, 1991) as a model system. At pH values below pH 3, this antibody adopts a stable conformation that is different from both the native and the denatured state. This A-state of the protein cannot be viewed as resulting from the native structure, e.g., by consecutive or continuous loosening of tertiary contacts. This is clearly demonstrated by the abrupt changes observed in the pH dependence of the transition temperatures of the various subtransitions (Figure 7). At neutral pH, five subtransitions can be identified, which are characterized by T_m values ranging from 80 to 63 °C. These subtransitions probably reflect the consecutive melting of different domains. Below about pH 4, two transitions vanish and only the three remaining subtransitions exhibit the normal decrease of T_m.

At pH < 3, a new stable structure appears that cannot be predicted on the basis of the behavior above pH 3. This low-pH structure (A-state), which exhibits two subtransitions on thermal unfolding, with T_m values at about 67 and 72 °C and corresponding ΔH values of 335 and 347 kJ/mol, does not exist at higher pH values. Therefore, the protonation of amino acids containing acidic side chains is probably decisive for the reorganization of structure. The A-state must be stabilized by well-defined tertiary contacts comparable to those found in native proteins. This conclusion can be drawn on the basis of the high cooperativity of the thermal- and GdmCl-induced unfolding transitions (3.3 M GdmCl for MAK33 in the A-state at pH 2). Additional support for the existence of significant interactions in the unique structure below pH 3 is provided by the magnitude of the specific transition enthalpy of the protein. The Δh values listed in Table II are comparable with those of other small globular proteins at pH 7 (Pfeil, 1986). Although there is a considerable decrease in Δh in lowering the pH to pH 2, the residual value of approximately 5 J/g is still sufficiently large for maintaining short- and long-range interactions, as revealed by the cooperativity of the unfolding transition.

The compactness of the A-state is further corroborated by sedimentation analysis. The apparent sedimentation coefficients of IgG in its A-state are close to the value observed for the native protein. Correcting for charge effects results in a slightly lower $s_{20,w}$ value for the A-state compared to the native antibody (Table I). However, the limiting value still corresponds to standard values of common globular proteins [Sober, 1970; cf. Jaenicke et al. (1968)].

CD spectra in the far-UV region clearly show that the secondary structure is rearranged at pH 2. On the basis of the present results, it cannot be decided whether the increase in the negative ellipticity of the A-state as compared to native IgG at pH 7 reflects formation of α-helices instead of an all-β-sheet conformation. As an alternative explanation for the increase in negative ellipticity, a change in the environment of aromatic amino acids could be visualized, since tyrosine and tryptophan have strong positive CD peaks in the far-UV region (Brahms & Brahms, 1980; Khan et al., 1989). Furthermore, in the native stae at pH 7 the fluorescence of immunoglobulins is quenched by adjacent disulfide bonds (Cowgill, 1967; Tsunegawa, 1987). The increase in fluorescence intensity at pH 2 shows that quenching does not occur in the acid-specific conformation. However, the maximum of fluorescence emission is identical at both pH 7 and pH 2. This result implies that the environment of the aromatic amino acid residues is different but has similar polarity in both cases.

The complex slow and multiphasic folding transition from the native to the A-state indicates that there is no simple switch in conformation. It has to be assumed that large-scale reshuffling processes are involved. In the folding kinetics from the unfolded state to the A-state both fast and slow folding steps can be clearly separated: about 85% of the fluorescence change occurs within the first second of refolding while the remaining 15% of the fluorescence signal are regained in slow reactions. This clearly distinguishes the A-state from the *molten globule* state. A basic characteristic of the *molten globule* state is that it exists in a rapid equilibrium with the unfolded state. All observed kinetics from the unfolded state to the *molten globule* state have relaxation times in the millisecond time range (Kuwajima, 1989). Thus, one may conclude that the fast reactions reflect the formation of a *molten globule* like intermediate that is separated from the A-state by an activation barrier.

Although the CD spectrum of the A-state in the near-UV range does not show pronounced features of tertiary structure, the highly cooperative transitions observed for both temperature and GdmCl unfolding indicate that well-defined tertiary contacts are present. This structural feature has so far never been observed with proteins that adopt the *molten globule* state. Since the environment of the aromatic amino acids is different in the A-state compared to the native state (as judged by the intrinsic fluorescence), it seems that low pH gives rise to tertiary contacts that are distinct from those found in the native state.

The present data clearly show that immunoglobulins adopt a specific, stable structure at low pH values. This alternatively folded A-state contains characteristics that are typical both for native proteins and for *molten globule* structures.

The native state of a protein is the result of evolutionary selection for optimal function and stability under physiological conditions. It is thought to be the unique stable structure of a given amino acid sequence. The conformational stability governed by hydrophobic effects and electrostatic and van der Waals interactions is usually very low. Small changes of these interactions such as the protonation of side chains (e.g., by lowering the pH) normally results in a decreased stability of the protein and can even lead to the complete loss of ordered structure.

Here we show that the formation of an alternatively folded structure different from the native state is possible upon the

protonation of acidic side chains. Other small changes such as mutations, insertions, deletions, etc., could similarly result in an "alternatively folded" structure as compared to the wild-type conformation. New folding motifs could evolve from these structures.

ACKNOWLEDGMENTS

We gratefully acknowledge the excellent technical assistance of Karla Lehle. We are indebted to Roman Meyer for performance of the density measurements.

REFERENCES

Amzel, L. M., & Poljak, R. J. (1979) *Annu. Rev. Biochem. 48*, 961–997.
Baldwin, R. L. (1990) *Nature 346*, 409–410.
Bevington, P. R. (1969) *Data Reduction and Error Analysis for the Physical Sciences*, McGraw-Hill, New York.
Brahms, S., & Brahms, J. (1980) *J. Mol. Biol. 138*, 149–178.
Brandts, J. F., & Lin, L.-N. (1990) *Biochemistry 29*, 6927–6940.
Buchner, J., & Rudolph, R. (1991) *Bio/Technology 9*, 157–162.
Buckel, P., Hübner-Parajsz, C., Mattes, R., Lenz, H., Haug, H., & Beaucamp, K. (1987) *Gene 51*, 13–19.
Cowgill, R. W. (1967) *Biochim. Biophys. Acta 140*, 37–44.
Damaschun, G., Gernat, C., Damaschun, H., Bychkova, V. E., & Ptitsyn, O. B. (1986) *Int. J. Biol. Macromol. 8*, 226–230.
Davies, D. R., & Metzger, H. (1983) *Annu. Rev. Immunol. 1*, 87–117.
Dill, K. A. (1990) *Biochemistry 29*, 7133–7155.
Dolgikh, D. A., Abaturov, L. V., Bolotina, I. A., Brazhnikov, E. V., Bychkova, V. E., Bushuev, V. N., Gilmanshin, R. I., Lebedev, Y. O., Semisotnov, G. V., Tiktopulo, E. I., & Ptitsyn, O. B. (1985) *Eur. Biophys. J. 13*, 109–121.
Engelhard, M., Rudolph, R., & Jaenicke, R. (1976) *Eur. J. Biochem. 67*, 447–453.
Freire, E., & Biltonen, R. (1978) *Biopolymers 17*, 463–479.
Gast, K., Zirwer, D., Welfle, H., Bychkova, V. E., & Ptitsyn, O. B. (1986) *Int. J. Biol. Macromol. 8*, 287–291.
Goloubinoff, P., Christeller, J. T., Gatenby, A. A., & Lorimer, G. (1989) *Nature 342*, 884–889.
Goto, Y., & Fink, A. (1989) *Biochemistry 28*, 945–952.
Goto, Y., & Hamaguchi, K. (1982) *J. Mol. Biol. 156*, 891–910.
Goto, Y., Azuma, T., & Hamaguchi, K. (1979) *J. Biochem. 85*, 1427–1438.
Goto, Y., Tsunenaga, M., Kawata, Y., & Hamaguchi, K. (1987) *J. Biochem. 101*, 319–329.
Goto, Y., Calciano, L. J., & Fink, A. L. (1990a) *Proc. Natl. Acad. Sci. U.S.A. 87*, 573–577.
Goto, Y., Takahashi, N., & Fink, A. L. (1990b) *Biochemistry 29*, 3480–3488.
Jaenicke, R. (1987) *Prog. Biophys. Mol. Biol. 49*, 117–237.
Jaenicke, R. (1991) *Biochemistry 30*, 3147–3161.
Jaenicke, R., Schmid, D., & Knof, S. (1968) *Biochemistry 7*, 919–929.
Jiang, J. X., & London, E. (1990) *J. Biol. Chem. 265*, 8636–8641.
Kauzmann, W. (1959) *Adv. Protein Chem. 14*, 1–67.
Khan, M. Y., Villanueva, G., & Newman, S. A. (1989) *J. Biol. Chem. 264*, 2139–2142.
Kiefhaber, T., Schmid, F. X., Renner, M., Hinz, H.-J., Hahn, U., & Quaas, R. (1990) *Biochemistry 29*, 8250–8257.
Kikuchi, H., Goto, Y., & Hamaguchi, K. (1986) *Biochemistry 25*, 2009–2013.
Kim, P. S., & Baldwin, R. L. (1990) *Annu. Rev. Biochem. 59*, 631–660.
Koynova, R., & Hinz, H.-J. (1990) *Chem. Phys. Lipids 54*, 67–72.
Kronman, M. J., Cerankowski, L., & Holmes, L. G. (1965) *Biochemistry 4*, 518–525.
Kronman, M. J., Holmes, L. G., & Robbins, F. M. (1967) *Biochim. Biophys. Acta 133*, 46–55.
Kuwajima, K. (1989) *Proteins: Struct., Funct., Genet. 6*, 87–103.
Kuwajima, K., Ogawa, Y., & Sugai, S. (1981) *J. Biochem. 89*, 759–770.
Mulqueen, P. M., & Kronman, M. J. (1982) *Arch. Biochem. Biophys. 215*, 28–39.
Moses, E., & Hinz, H.-J. (1983) *J. Mol. Biol. 170*, 285–317.
McCoy, L. F., & Wong, K.-P. (1981) *Biochemistry 20*, 3062–3067.
Pace, C. N. (1986) *Methods Enzymol. 131*, 266–280.
Pfeil, W. (1986) in *Thermodynamic Data for Biochemistry and Biotechnology* (Hinz, H.-J., Ed.) pp 349–399, Springer Verlag, Berlin.
Privalov, P. L. (1979) *Adv. Protein Chem. 33*, 167–241.
Privalov, P. L., & Gill, S. J. (1988) *Adv. Protein Chem. 39*, 191–234.
Privalov, P. L., Plotnikov, V. V., & Filimonov, V. V. (1975) *J. Chem. Thermodyn. 7*, 41–47.
Ptitsyn, O. B. (1987) *J. Protein Chem. 6*, 273–293.
Ptitsyn, O. B., Pain, R. H., Semisotnov, G. V., Zerovnik, E., & Razgulyaev, O. I. (1990) *FEBS Lett. 262*, 20–24.
Renner, M. (1991) Dissertation, University of Regensburg.
Rudolph, R., Holler, E., & Jaenicke, R. (1975) *Biophys. Chem. 3*, 226–233.
Rudolph, R., Neβlauer, G., Siebendritt, R., Sharma, A. K., & Jaenicke, R. (1990) *Proc. Natl. Acad. Sci. U.S.A. 87*, 4625–4629.
Sackett, D. L., & Wolff, J. (1987) *Anal. Biochem. 167*, 228–234.
Schwarz, H., Hinz, H.-J., Mehlich, A., Tschesche, H., & Wenzel, H. (1987) *Biochemistry 26*, 3544–3551.
Sober, H. A., Ed. (1970) *Handbook of Biochemistry*, 2nd ed., p C10, CRC, Cleveland, OH.
Sturtevant, J. M. (1987) *Annu. Rev. Phys. Chem. 38*, 463–488.
Svedberg, T., & Pedersen, K. O. (1940) in *Die Ultrazentrifuge* p 32, Dr. T. Steinkopff Verlag, Dresden and Leipzig.
Tanford, C. (1968) *Adv. Protein Chem. 23*, 122–282.
Tsunegawa, M., Goto, Y., Kawata, Y., & Hamaguchi, K. (1987) *Biochemistry 26*, 6044–6051.
Wetlaufer, D. B. (1962) *Adv. Protein Chem. 17*, 303–390.
Yphantis, D. A. (1964) *Biochemistry 3*, 297–310.
Zettlmeissl, G., Rudolph, R., & Jaenicke, R. (1981) *Eur. J. Biochem. 121*, 169–175.